

Supporting Information

# NiAg<sub>0.4</sub> 3D porous nanoclusters with epitaxial interfaces exhibiting Pt like activity towards hydrogen evolution in alkaline medium

Chidanand Hegde,<sup>‡a</sup> Xiaoli Sun,<sup>‡b</sup> Hao Ren,<sup>c</sup> Aijian Huang,<sup>d</sup> Daobin Liu,<sup>c</sup> Bing Li,<sup>e</sup> Raksha Dangol,<sup>c</sup> Chuntai Liu,<sup>f</sup> Shuiqing Li,<sup>\*b</sup> Hua Li<sup>\*a</sup> and Qingyu Yan<sup>\*c</sup>

<sup>a</sup>Singapore Center for 3D Printing, Department of Mechanical and Aerospace Engineering, Nanyang Technological University, Singapore 639798, Singapore

<sup>b</sup>Department of Energy and Power Engineering, Tsinghua University, Beijing, 100084, China

<sup>c</sup>Department of Materials Science and Engineering, Nanyang Technological University, Singapore 639798, Singapore

<sup>d</sup>School of Electronics Science and Engineering, University of Electronic Science and Technology of China, Chengdu, 610054, P.R. China

<sup>e</sup>Institute of Materials Research and Engineering, A\*STAR (Agency for Science, Technology, and Research), 2 Fusionopolis Way Innovis #08-03, Singapore 138634, Singapore

<sup>f</sup>Key Laboratory of Materials Processing and Mold, Ministry of Education, Zhengzhou University, Zhengzhou 450002, China

\*Corresponding authors.

E-mail addresses: [alexyan@ntu.edu.sg](mailto:alexyan@ntu.edu.sg) (Q. Yan), [lishuiqing@mail.tsinghua.edu.cn](mailto:lishuiqing@mail.tsinghua.edu.cn) (S. Li), [lihua@ntu.edu.sg](mailto:lihua@ntu.edu.sg) (H. Li).

<sup>‡</sup>These authors contributed equally.

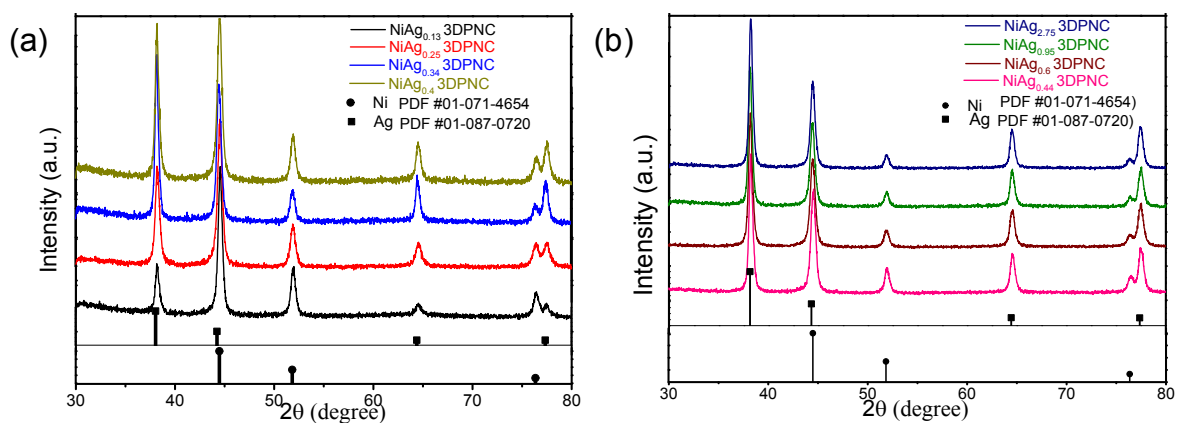


**Fig. S1** XRD patterns of (a)  $\text{NiAg}_{0.13}$  3DPNC,  $\text{NiAg}_{0.25}$  3DPNC,  $\text{NiAg}_{0.34}$  3DPNC, and  $\text{NiAg}_{0.4}$  3DPNC, and (b)  $\text{NiAg}_{0.44}$  3DPNC,  $\text{NiAg}_{0.6}$  3DPNC,  $\text{NiAg}_{0.95}$  3DPNC, and  $\text{NiAg}_{2.75}$  3DPNC.

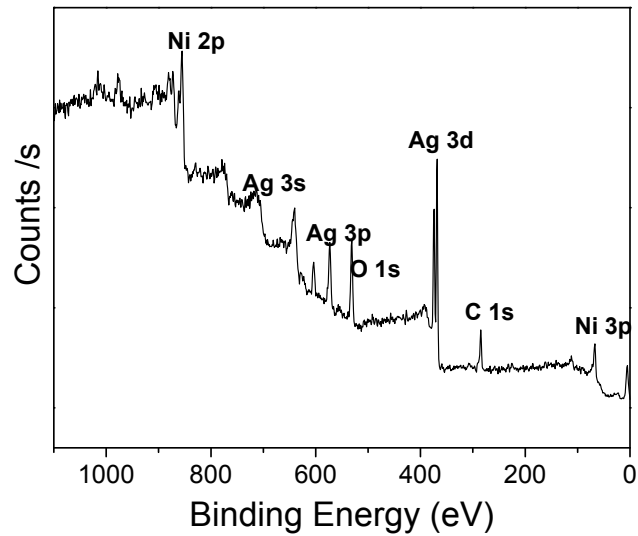


**Fig. S2** XPS survey spectrum of  $\text{NiAg}_{0.4}$  3DPNC.

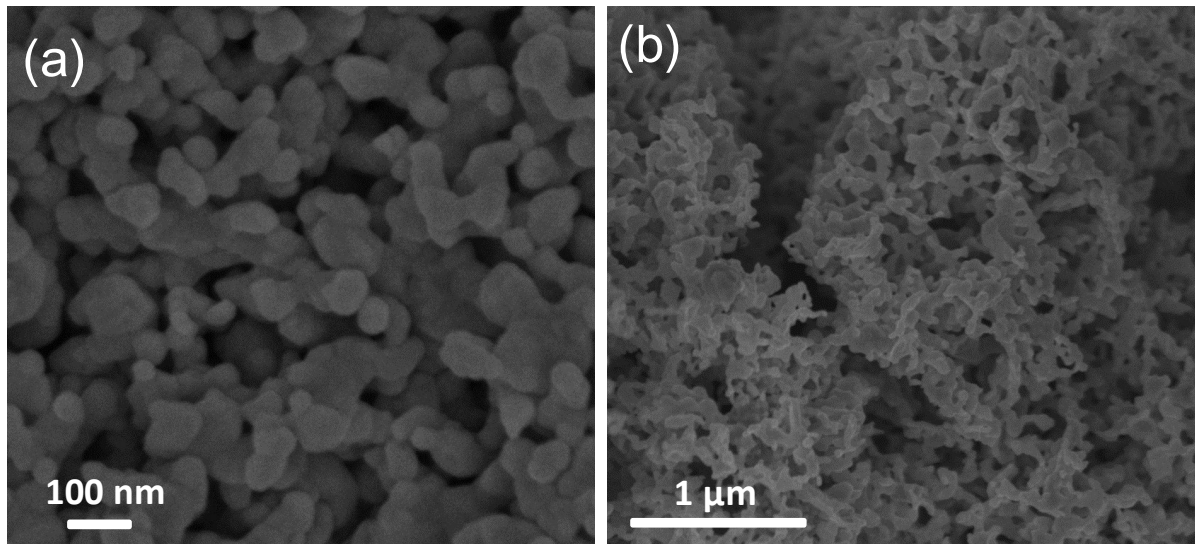


**Fig. S3** FESEM images of (a) Ag NPs, (b) Ni 3DPNC.

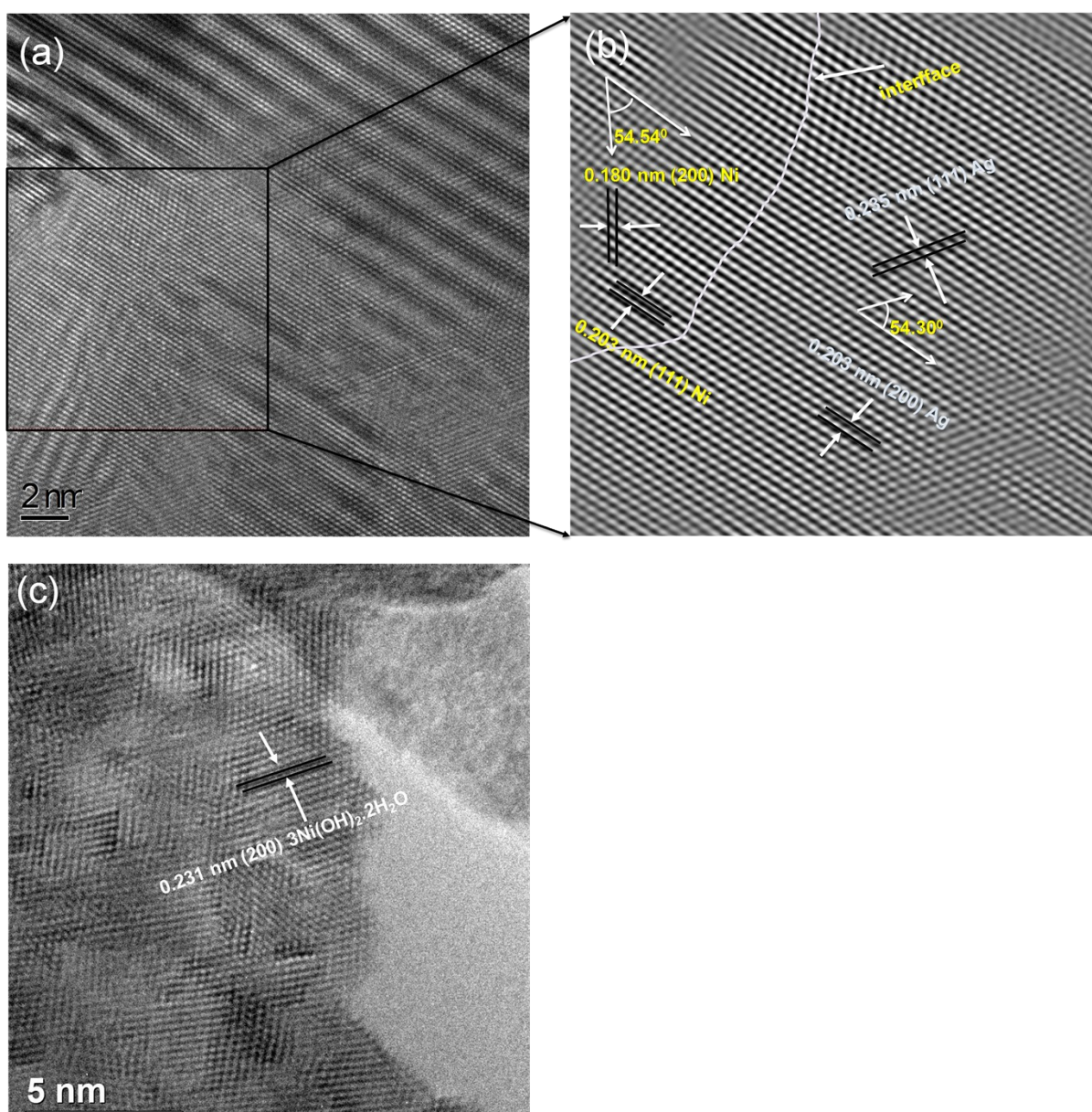


**Fig. S4** HRTEM image of (a)  $\text{NiAg}_{0.4}$  3DPNC, (b) FFT analyzed image of  $\text{NiAg}_{0.4}$  3DPNC, and (c) HRTEM image of  $\text{Ag}/\text{Ni}(\text{OH})_2 \cdot 2/3\text{H}_2\text{O}$  precursor.

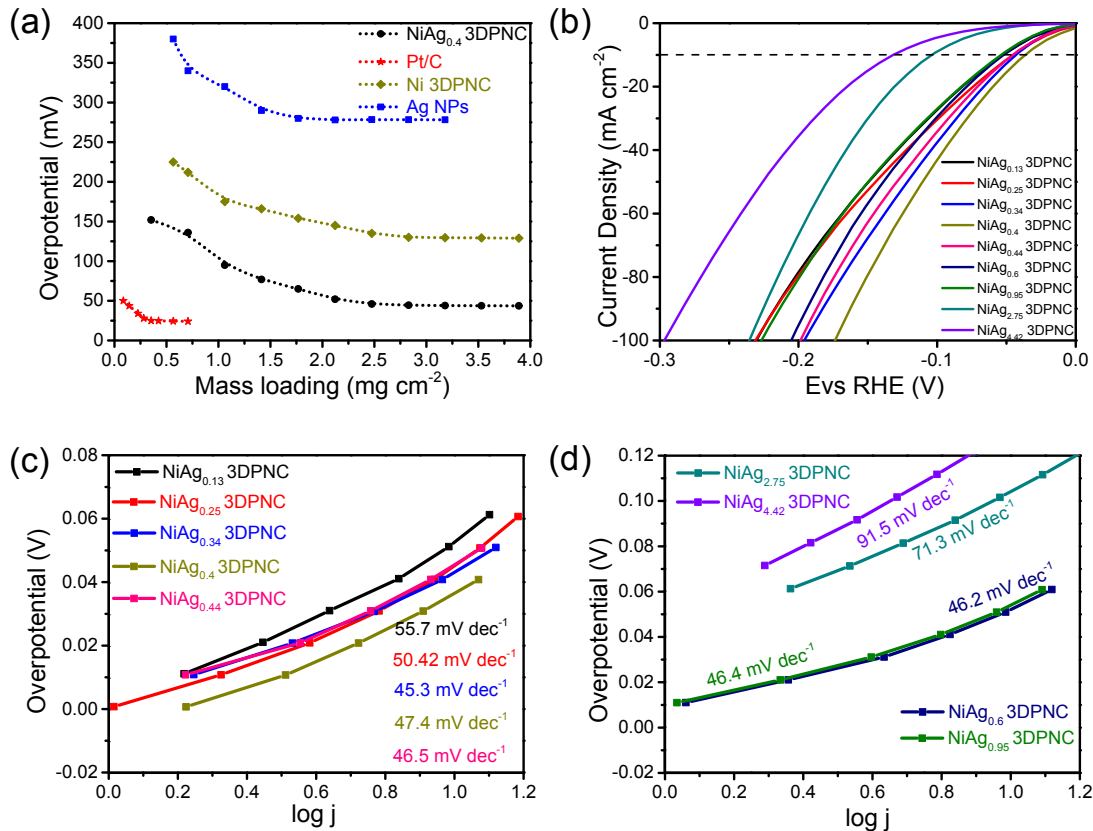


**Fig. S5** (a) Variation of overpotential with catalyst loading for Ni 3DPNC, Ag NPs, NiAg<sub>0.4</sub> 3DPNC, and Pt/C catalysts. (b) HER polarization curves of NiAg<sub>x</sub> 3DPNC with varying Ni to Ag ratios without iR correction and their corresponding (c-d) Tafel plots.

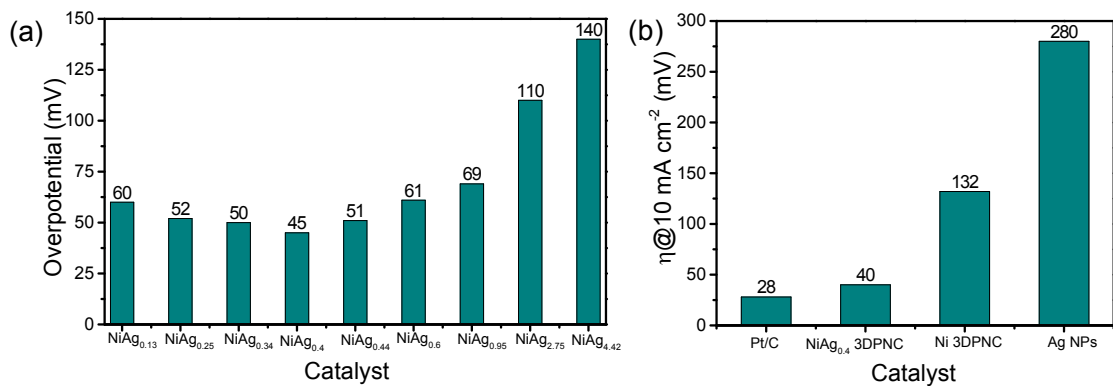


**Fig. S6** Variation of overpotential at  $10 \text{ mA cm}^{-2}$  for (a) synthesized catalysts with varying Ag composition, (b) Pt/C,  $\text{NiAg}_{0.4}$  3DPNC, Ni 3DPNC and Ag NPs.

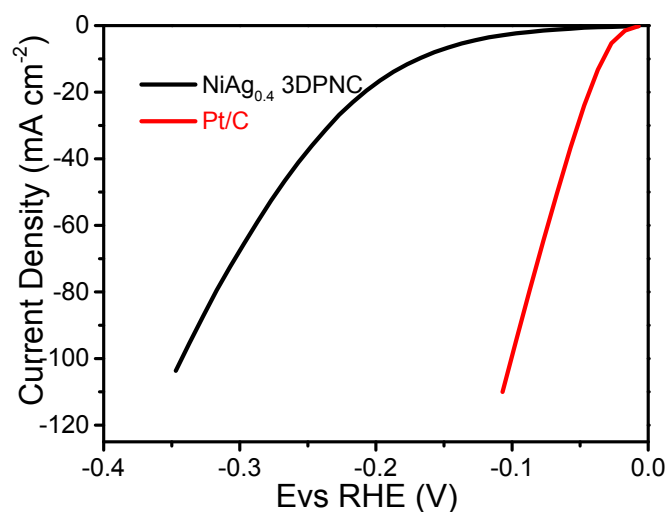


**Fig. S7** HER polarization curves for  $\text{NiAg}_{0.4}$  3DPNC and Pt/C in  $0.5 \text{ M H}_2\text{SO}_4$ .

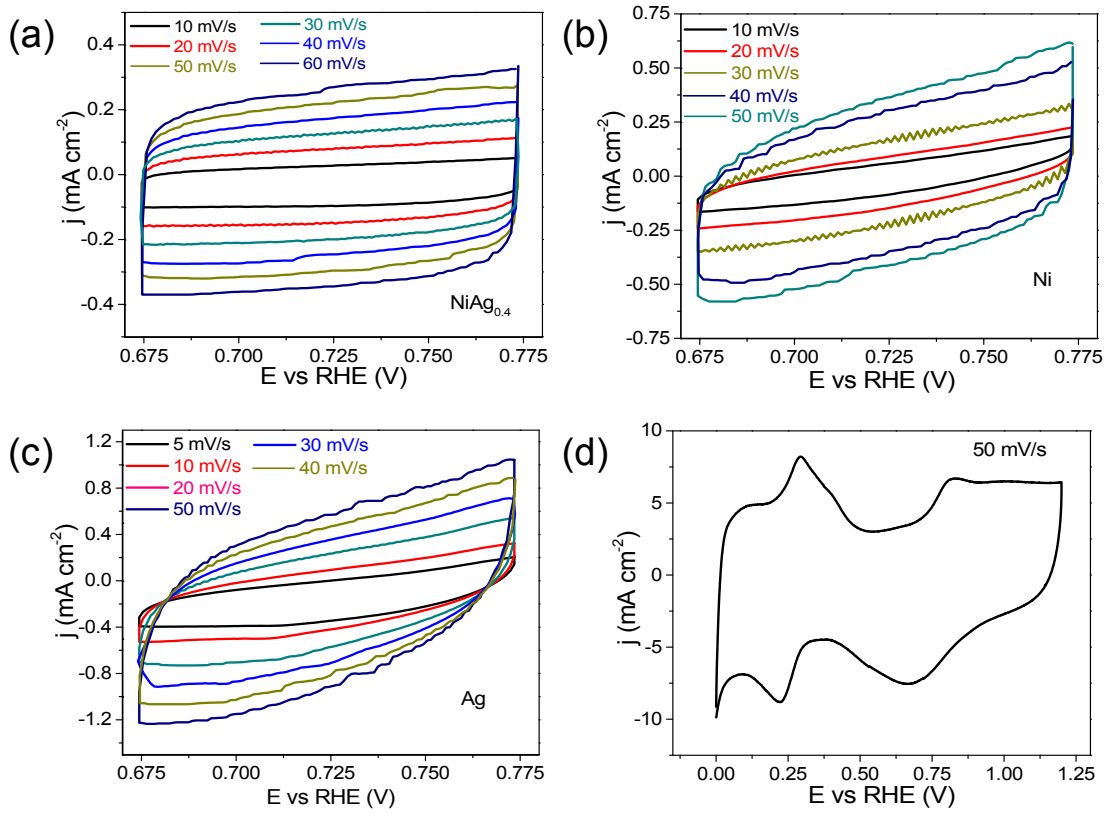


**Fig. S8** Cyclic voltammogram (CV) curves for (a)  $\text{NiAg}_{0.4}$  3DPNC, (b) Ni 3DPNC, (c) Ag NPs, and (d) CV curve for underpotential deposition for Pt/C 20% wt. catalyst.

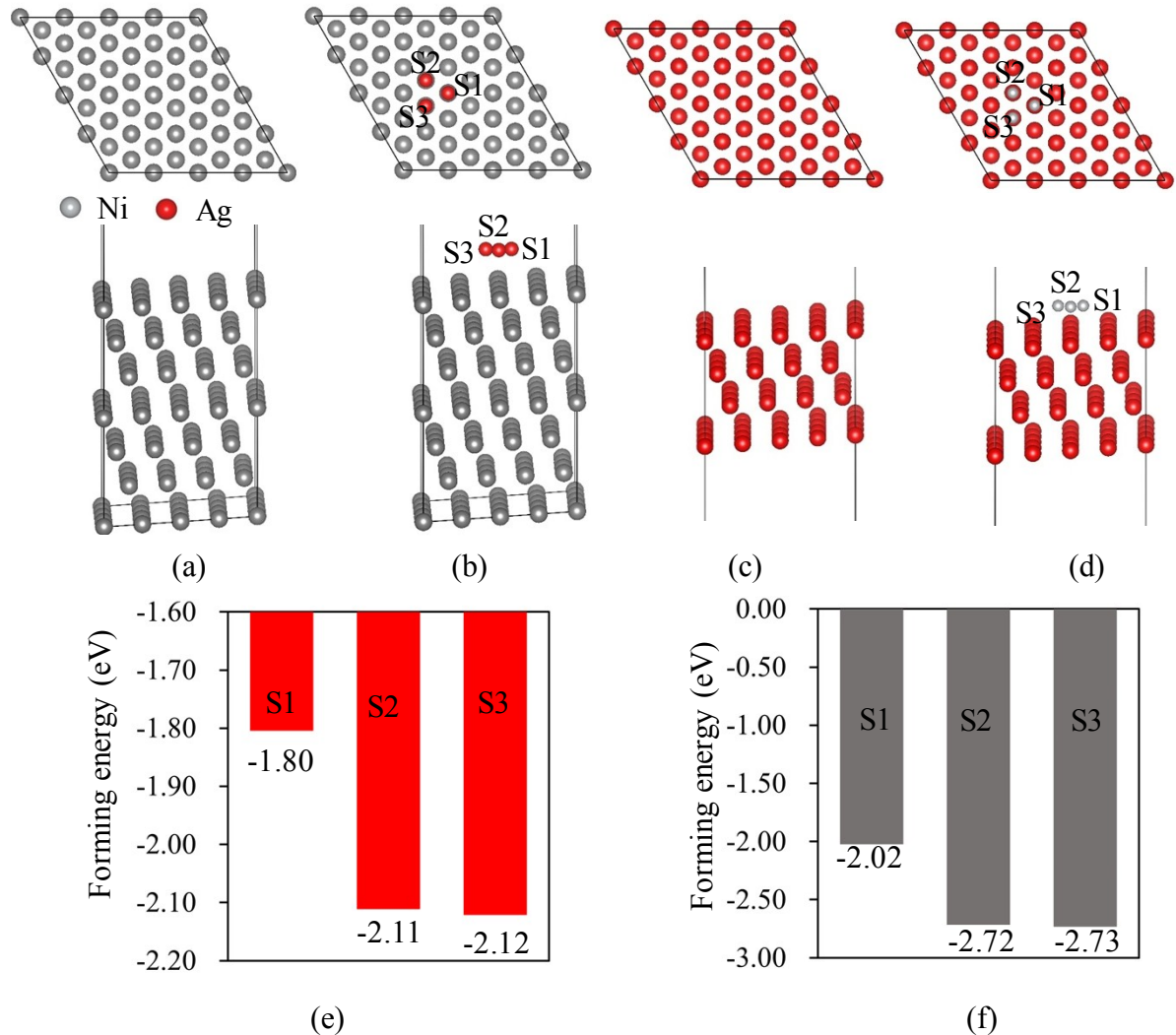


**Fig. S9** The top and side view of crystal structures of: (a) pristine Ni (111) surface, (b) Ag/Ni (111) surface where the adsorption sites: top of Ni (S1), the Ni fcc sites (S2) and Ni hcp sites (S3); the top and side view of crystal structures of (c) pristine Ag (111) surface, (b) Ni/Ag (111) surface where the adsorption sites: top of Ag (S1), the Ag fcc sites (S2) and Ag hcp sites (S3); (e) the forming energy of Ag adsorbed on Ni (111) surface; (f) the forming energy of Ni adsorbed on Ag(111) surface.

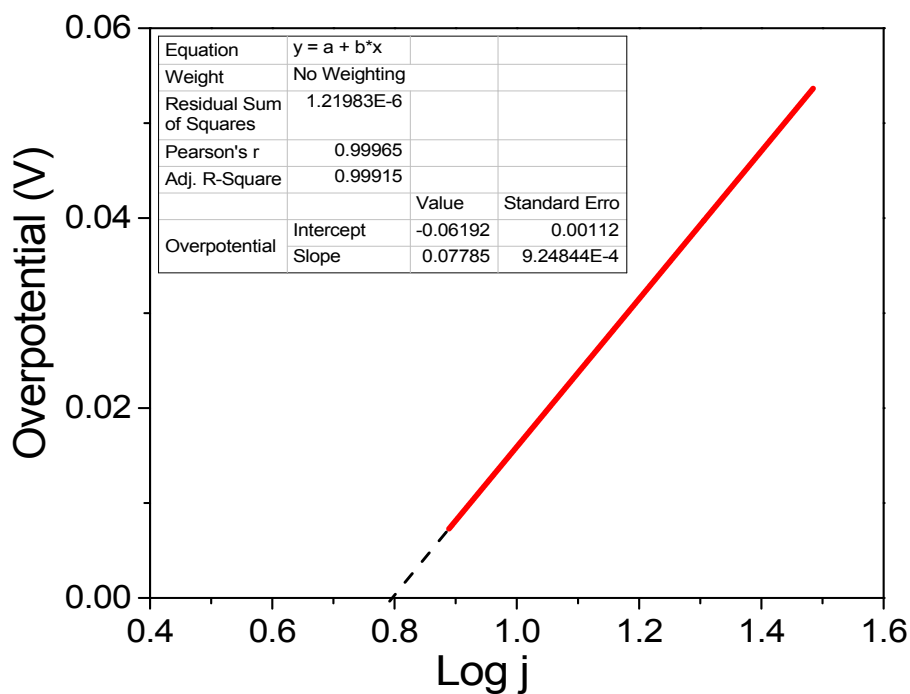


**Fig. S10** Tafel plot of NiAg<sub>0.4</sub> 3DPNC to evaluate the exchange current density. Exchange current density was computed from the Tafel equation.

The exchange current density of the NiAg<sub>0.4</sub> 3DPNC based on the geometric surface area was computed from the Tafel equation as shown below:

$$\eta = -0.062 + 0.077 \log j$$

$$0 = -0.062 + 0.077 \log j$$

$$\log j = 0.8052$$

$$j_0_{\text{geometric}} = 6.3856 \text{ mA cm}^{-2}_{\text{geometric}}$$

$$j_0_{(\text{ECSA})} = 6.3856 / 125 \text{ mA cm}^{-2}_{(\text{ECSA})}$$

$$j_0_{(\text{ECSA})} = 5.10 * 10^{-5} \text{ A cm}^{-2}_{(\text{ECSA})}$$

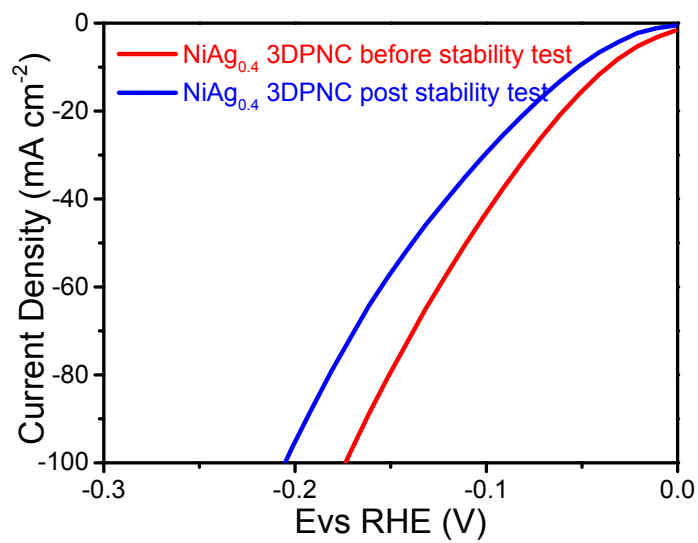


**Fig. S11** Comparison of HER polarization curve of  $\text{NiAg}_{0.4}$  3DPNC after 80 hours chronoamperometry test with the initial catalyst.

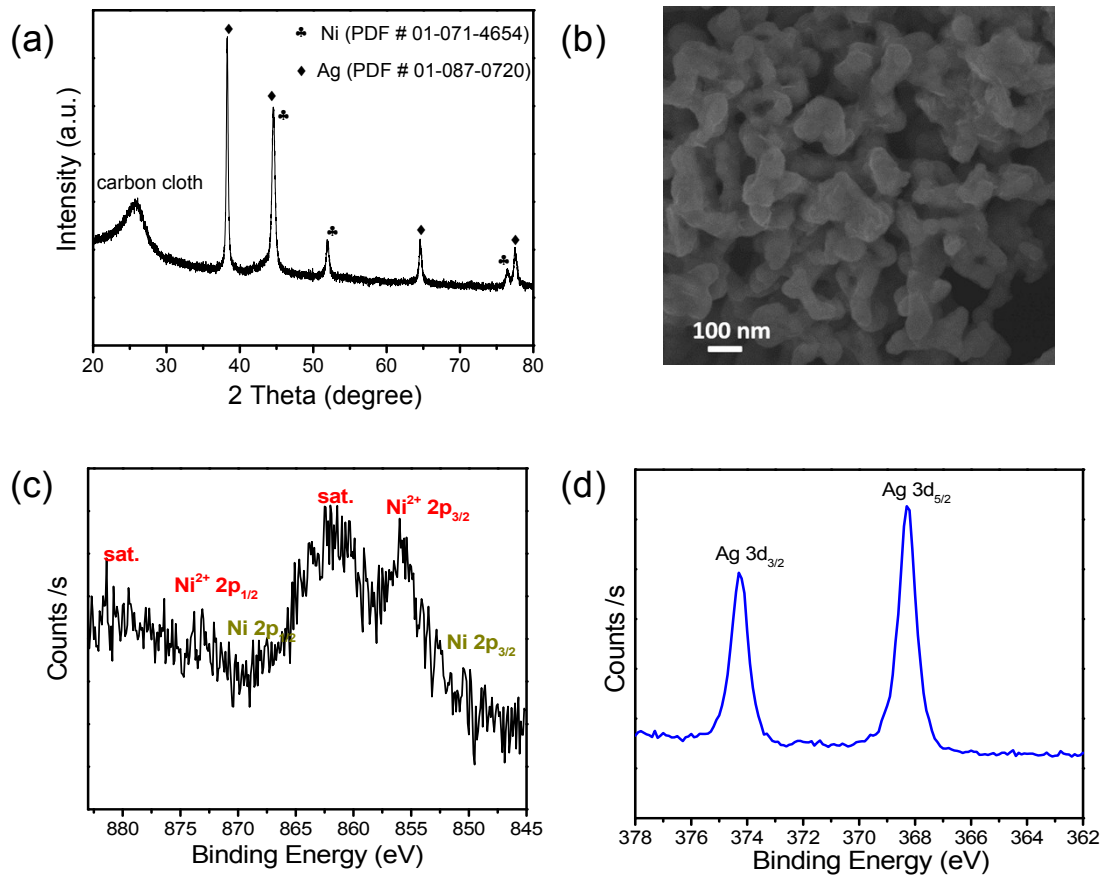


**Fig. S12** (a) XRD pattern of  $\text{NiAg}_{0.4}$  3DPNC after 80 hours chronoamperometry test. (b) FESEM image of the  $\text{NiAg}_{0.4}$  3DPNC after chronoamperometry test. XPS spectra of  $\text{NiAg}_{0.4}$  3DPNC after 80 hours chronoamperometry test in the (c) Ni 2p region, (d) Ag 3d region.

**Table S1.** Inductive couple plasma- atomic emission spectroscopy results for the synthesized samples with different Ni/Ag ratios.

Ni : Ag ratio in the precursor solution	Expected molar concentration from synthesis	Measured molar concentration from ICP-OES	Expected molar concentration from synthesis	Measured molar concentration from ICP-OES	Sample name in the report
	Ni (%)	Ni (%)	Ag (%)	Ag (%)	
1 : 0.1	90.9	88.43019	9.1	11.56981	NiAg <sub>0.13</sub> 3DPNC
1 : 0.2	83	80.20356	17	19.79644	NiAg <sub>0.25</sub> 3DPNC
1 : 0.3	76.9	74.63433	23.1	25.36567	NiAg <sub>0.34</sub> 3DPNC
1 : 0.4	71.5	71.89	28.5	28.11	NiAg <sub>0.4</sub> 3DPNC
1 : 0.5	66.67	69.57572	33.33	30.42428	NiAg <sub>0.44</sub> 3DPNC
1 : 0.6	62.5	62.55256	37.5	37.44744	NiAg <sub>0.6</sub> 3DPNC
1 : 0.8	55.55	51.37111	44.45	48.62889	NiAg <sub>0.95</sub> 3DPNC
1 : 2	33.33	26.63245	66.67	73.36755	NiAg <sub>2.75</sub> 3DPNC
1 : 3	25	18.4579	75	81.5421	NiAg <sub>4.42</sub> 3DPNC
		68.5		31.5	NiAg <sub>0.4</sub> 3DPNC Post chronoamperometry test

**Table S2.** Roughness factor values for different catalysts which was evaluated from the double layer capacitance.

Catalyst	C <sub>dl</sub> (mF cm <sup>-2</sup> )	Roughness factor (cm <sup>2</sup> per cm <sup>2</sup> <sub>(geometric)</sub> )
Ni 3DPNC	7	175
Ag NPs	12.8	320
Pt/C	20.4738 mC cm <sup>-2</sup>	97.5
NiAg <sub>0.4</sub> 3DPNC	4.9	125

**Table S3.** HER activity of the NiAg<sub>0.4</sub>3DPNC in comparison with other recently reported catalysts with good activity.

Catalyst	HER overpotential (mV@mA cm <sup>-2</sup> )	Tafel slope (mV dec <sup>-1</sup> )	Electrolyte	Stability	Reference
Boron doped RhFe alloy	25 mV @ 10 mA cm <sup>-2</sup>	32	0.5 M H <sub>2</sub> SO <sub>4</sub>	8 hours	<sup>1</sup>
Ni <sub>20</sub> Fe <sub>20</sub> Mo <sub>10</sub> Co <sub>35</sub> Cr <sub>15</sub> high entropy alloy	172 mV @ 10 mA cm <sup>-2</sup>	41	1 M KOH	8 hours	<sup>2</sup>
Pt <sub>3</sub> Ni <sub>3</sub> NWs	70 mV @ 19.8 mA cm <sup>-2</sup>	NA	1 M KOH	3 hours	<sup>3</sup>
Micro-nano MoS <sub>2</sub> spheres	214 mV @ 10 mA cm <sup>-2</sup>	74	0.5 M H <sub>2</sub> SO <sub>4</sub>	24 hours	<sup>4</sup>
Pt <sub>3</sub> Co nanoparticles	32.6 mV @ 10 mA cm <sup>-2</sup>	28.6	0.5 M H <sub>2</sub> SO <sub>4</sub>	5000 CV cycles	<sup>5</sup>
np-CoP <sub>3</sub> on Ti mesh	76 mV @ 10 mA cm <sup>-2</sup>	50	1 M KOH	60 hours	<sup>6</sup>
PtCo–Co/TiM	70 mV @ 46.5 mA cm <sup>-2</sup>	35	1 M KOH	50 hours	<sup>7</sup>
Fe <sub>1.89</sub> Mo <sub>4.11</sub> O <sub>7</sub> /MoO <sub>2</sub>	197 mV @ 10 mA cm <sup>-2</sup>	79	1 M KOH	1000 CV cycles	<sup>8</sup>
V-doped Ni <sub>3</sub> S <sub>2</sub> Nanowires on Ni foam	68 mV @ 10 mA cm <sup>-2</sup>	112	1 M KOH	7000 cycles	<sup>9</sup>

CrO <sub>x</sub> /Ni–Cu	48 mV @ 10 mA cm <sup>-2</sup>	64	KH <sub>2</sub> PO <sub>4</sub> + K <sub>2</sub> HPO <sub>4</sub> buffer (pH = 7)	24 hours	10
FeP nanoparticles	154 mV @ 10 mA cm <sup>-2</sup>	65	0.5 M H <sub>2</sub> SO <sub>4</sub>	1.66 hours	11
IrAg nanotubes	20 mV @ 10 mA cm <sup>-2</sup>	61.1	0.5 M H <sub>2</sub> SO <sub>4</sub>	6 hours	12
<b>NiAg<sub>0.4</sub>3DPNC</b>	<b>40 mV @ 10 mA cm<sup>-2</sup></b>	<b>39.1</b>	<b>1 M KOH</b>	<b>80 hours and 5000 CV cycles</b>	<b>This work</b>

---

## References

- 1 L. Zhang, J. Lu, S. Yin, L. Luo, S. Jing, A. Brouzgou, J. Chen, P. K. Shen and P. Tsiaikaras, *App. Catal. B: Envir.*, 2018, **230**, 58-64.
- 2 G. Zhang, K. Ming, J. Kang, Q. Huang, Z. Zhang, X. Zheng and X. Bi, *Electrochim. Acta*, 2018, **279**, 19-23.
- 3 P. Wang, K. Jiang, G. Wang, J. Yao and X. Huang, *Angew. Chem.*, 2016, **55**, 12859-12863.
- 4 B. Guo, K. Yu, H. Li, H. Song, Y. Zhang, X. Lei, H. Fu, Y. Tan and Z. Zhu, *ACS App. Mater. Interfaces*, 2016, **8**, 5517-5525.
- 5 Z. Cheng, X. Geng, L. Chen, C. Zhang, H. Huang, S. Tang and Y. Du, *J. Mater. Sci.*, 2018, **53**, 12399-12406.
- 6 Y. Ji, L. Yang, X. Ren, G. Cui, X. Xiong and X. Sun, *ACS Sustain. Chem. Eng.*, 2018, **6**, 11186-11189.
- 7 Z. Wang, X. Ren, Y. Luo, L. Wang, G. Cui, F. Xie, H. Wang, Y. Xie and X. Sun, *Nanoscale*, 2018, **10**, 12302-12307.
- 8 Z. Hao, S. Yang, J. Niu, Z. Fang, L. Liu, Q. Dong, S. Song and Y. Zhao, *Chem. Sci.*, 2018, **9**, 5640-5645.
- 9 Y. Qu, M. Yang, J. Chai, Z. Tang, M. Shao, C. T. Kwok, M. Yang, Z. Wang, D. Chua, S. Wang, Z. Lu and H. Pan, *ACS Appl. Mater. Interfaces*, 2017, **9**, 5959-5967.
- 10 C.-T. Dinh, A. Jain, F. P. G. de Arquer, P. De Luna, J. Li, N. Wang, X. Zheng, J. Cai, B. Z. Gregory, O. Voznyy, B. Zhang, M. Liu, D. Sinton, E. J. Crumlin and E. H. Sargent, *Nat. Energy*, 2018, **4**, 107-114.
- 11 L. Tian, X. Yan and X. Chen, *ACS Catal.*, 2016, **6**, 5441-5448.
- 12 M. Zhu, Q. Shao, Y. Qian and X. Huang, *Nano Energy*, 2019, **56**, 330-337.